VIP Self-Assembly Processes

DOI: 10.1002/ange.200604012

Formation of Gels and Liquid Crystals Induced by Pt···Pt and π–π* Interactions in Luminescent σ-Alkynyl Platinum(II) Terpyridine Complexes**

Franck Camerel, Raymond Ziessel, Bertrand Donnio, Cyril Bourgogne, Daniel Guillon, Marc Schmutz, Cristian Iacovita, and Jean-Pierre Bucher*

Luminescent platinum–terpyridine or orthometalated bipyridine complexes have engendered widespread interest as functional materials, in particular stemming from their intense phosphorescence in the visible region of the electromagnetic spectrum.[1] These stable, neutral or ionic complexes have been widely used as electroluminescent thin films or as dopants in organic light-emitting devices (OLEDs),[2] as DNA intercalators,[3] and molecular probes for biological macromolecules.[4] In some cases, the ligand design,[5] the solvent,[6] or the use of soluble polymers induces metal···metal and π–π stacking interactions, which allow the tuning of the optical properties over a large spectral range.[7] Such intermolecular features are most useful for the engineering of liquid crystals and organogelators, for which intermolecular interactions are critical.[8]

Rodlike metal alkynyl complexes of Pd^{II}, Pt^{II}, Rh^{I}, and Hg^{I} exhibit thermotropic liquid-crystalline properties,[9] and metal–poly(yne) polymers form lyotropic liquid crystals.[10] However, as a result of the shape and anisotropy introduced by the alkynyl tethers, most of these complexes exhibit only lamellar (SmA) and nematic mesophases. Also, the absence of π-accepting chromophores results in non-luminescent materials, which notably limits their practical utilization in energy-conversion devices (OLEDs, solar cells, etc.). While phosphorescent organogels of quinolinol platinum(II) complexes have recently been characterized, there was no indication of metal···metal interactions that might provide an additional mechanism for the control of their properties.[11]

Thus, the construction of well-organized phosphorescent architectures remains an important objective, with the essential features being the need to incorporate 1) heavy metals to favor spin–orbit coupling for phosphorescence, 2) ligand tailoring to facilitate intermolecular interaction through hydrogen bonding (e.g. amide vectors) or π–π interactions through polyaromatic and/or polyimine fragments, and 3) d^8-transition metals which are known to favor square-planar structures, thus facilitating metal–metal interactions. Here, we disclose our results on organogels and mesomorphic materials obtained through such a strategy.

Syntheses of the pivotal ethynyl platforms **1a–c** were based on gallate-substituted derivatives with methyl, dodecyl ($C_{12}H_{25}$), or phytol-like ($C_{20}H_{41}$) substituents.[12] The final

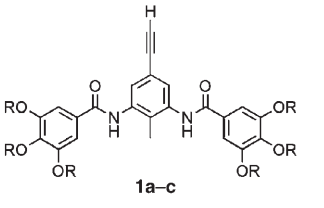

1a–c

a: R = CH_3

b: R =

c: R =

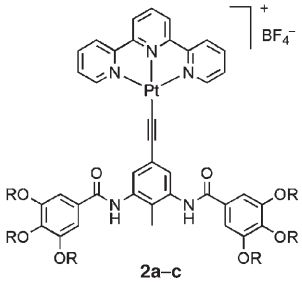

2a–c

complexes were prepared by a cross-coupling reaction under anaerobic conditions between the terminal ethynyl derivatives and $[(terpy)PtCl]BF_4$ (terpy = 2,2′:6′,6″-terpyridine).[13] The reaction is catalyzed by CuI (ca. 6 mol%), and triethylamine is required to quench the nascent HCl. The deep-red complexes **2a–c** were obtained in good yields after column chromatography and crystallization from a mixture of dichloromethane/methanol and further fully characterized by NMR and FTIR spectroscopy, ESI mass spectrometry, and elemental analysis.

[*] Dr. F. Camerel, Dr. R. Ziessel
Laboratoire de Chimie Moléculaire
ECPM, UMR 7509
CNRS – Université Louis Pasteur
25 rue Becquerel, 67087 Strasbourg Cedex 02 (France)
Fax: (+33) 3-9024-2689
E-mail: ziessel@chimie.u-strasbg.fr
Dr. B. Donnio, Dr. C. Bourgogne, Dr. D. Guillon, C. Iacovita, Prof. J.-P. Bucher
Institut de Physique et Chimie des Matériaux de Strasbourg (IPCMS)
Groupe des Matériaux Organiques (GMO), UMR 7504
CNRS – Université Louis Pasteur
23 rue du Loess, BP 43, 67034 Strasbourg Cedex 2 (France)
Dr. M. Schmutz
Institut Charles Sadron
CNRS – UPR 22
6 rue Boussingault, 67083 Strasbourg (France)

[**] This work was supported by the Centre National de la Recherche Scientifique and the Ministère de la Recherche et des Nouvelles Technologies. The authors thank Professor Jack Harrowfield (ISIS Strasbourg) for carefully reading and commenting on this manuscript prior to submission. We also thank Thomas Dombray for his help with the synthesis of the gallate derivatives with phytol-like substituents and Stéphane Diring for his contribution in the graphical design. We also warmly thank Johnson Matthey plc. for the loan of precious metals.

Supporting information for this article is available on the WWW under http://www.angewandte.org or from the author.

Compounds **2a**–**c** exhibit strong solvatochromism. Addition of methanol (7% v/v) to the deep-red solution of **2b** in dichloromethane ($\lambda_{max} = 487$ nm) results in the development of a yellow color, reflected in a hypsochromic shift of 17 nm in λ_{max}. In dodecane, a deep-green solution forms with the appearance of a new, strong absorption band at 644 nm, while the original intense metal-to-ligand charge-transfer (MLCT) band is bathochromically shifted by 11 nm (Figure 1a). An

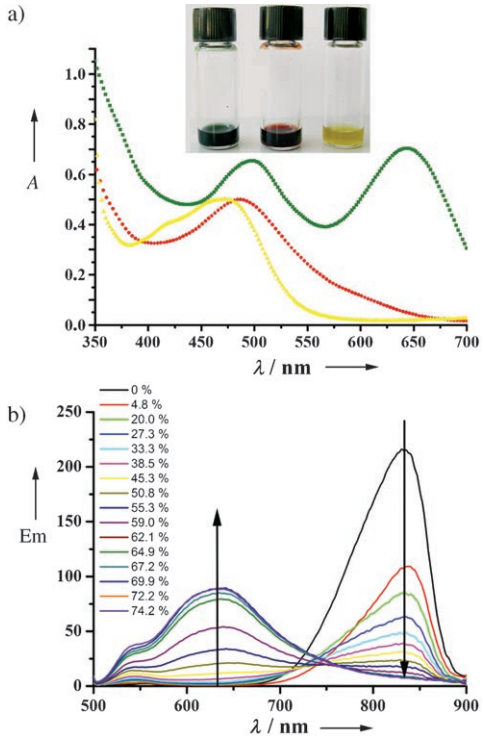

Figure 1. a) Absorption spectra of compound **2b** in dodecane ($c = 1.9\times10^{-4}$ mol L^{-1}; green line), in dichloromethane ($c = 1.9\times10^{-4}$ mol L^{-1}; red line), and in dichloromethane with 7% v/v methanol ($c = 1.01\times10^{-4}$ mol L^{-1}; yellow line). The inset shows a photograph of the corresponding solutions from left to right. b) Emission spectrum ($\lambda_{ex} = 482$ nm) of compound **2b** in dodecane ($c = 1.9\times10^{-4}$ mol L^{-1}) upon addition (% v/v) of a mixture of methanol (25% v/v) in dichloromethane.

unusually strong near-infrared emission is observed at 830 nm on irradiation of the dilute dodecane solution at 644 or 487 nm, and the excitation spectrum perfectly matches the absorption spectrum over the whole absorption range. Upon progressive addition of a mixture of methanol (25% v/v) in dichloromethane to the dodecane solution, the phosphorescent band at 850 nm gradually disappears and is replaced by an emission band at 635 nm (Figure 1b). This latter emission band is characteristic of that found for a solution in methanol/dichloromethane only. The strong absorption at 487 nm involves mixed dπ(Pt)→π*(terpy) MLCT and π(C≡)→π* (terpy) ligand-to-ligand charge-transfer (LLCT) transitions.[14] Likewise, the intense absorption at 644 nm may be assigned to a metal–metal–ligand charge-transfer (MMLCT) transition.[6] The intense emission observed at 644 nm in methanol/dichloromethane is assigned to a mixed ^{3}MLCT/^{3}LLCT state and that at 830 nm in pure dodecane is assigned to a ^{3}MMLCT state. On the basis of the assumption that the unusual dark-green color found in apolar dodecane could be caused by aggregation of the molecules favoring Pt···Pt, Pt···π, and π–π* stacking interactions, we were led to investigate the aggregation properties, in particular, their tendency to form gels. It was our aim to provide a simple entry to soft materials in which the local organization is driven by Pt···Pt and π–π* interactions.

Whereas complex **2a** is insoluble in alkanes, **2c** is highly soluble and no gels were produced under standard conditions. Compound **2b**, however, was found to be a good gelator of dodecane (minimum gelation concentration, MGC = 7.5 mmol L^{-1}). Dark-green gels (Figure 2a) displaying a

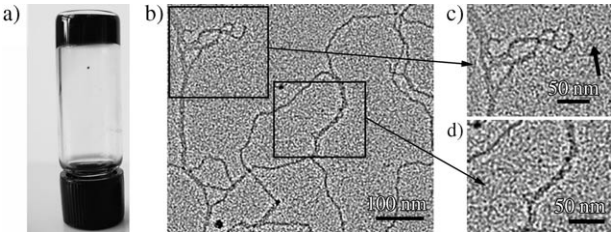

Figure 2. a) Gel obtained with **2b** in dodecane (8.1 mmol L^{-1}). The gel does not flow when the test tube is turned upside down. b) TEM image of a diluted gel of compound **2b** in dodecane ($c = 0.08$ mmol L^{-1}) showing an interconnected network of fibers. c) Zoom showing a fiber with the smallest observed diameter (2 nm; indicated by arrow). d) Zoom of intertwined bundles of fibers.

thermally reversible sol-to-gel phase transition were obtained from hot dodecane solutions. Modulation of the UV/Vis and static emission properties is feasible as a function of temperature to provide a deep-red liquid above 60 °C that turns back to the deep-green gelatinous state upon cooling to room temperature (Figure S2 in the Supporting Information). Infrared spectroscopy revealed that all C=O and NH functions are mutually hydrogen bonded in the gel (stretching vibrations at 1648 and 3379 cm^{-1}, respectively). These results are in line with similar observations made with 4-methyl-3,5-diacylaminophenyl platforms equipped with 2,2′:6′,2″-terpyridine ligands.[12a]

Images obtained from transmission electron microscopy (TEM) experiments on a diluted gel of compound **2b** in dodecane (0.08 mmol L^{-1}) dried onto a carbon-coated copper grid revealed the presence of an extended network of interlocked fibers responsible for the immobilization of the solvent (Figure 2b). The contrast of the structures is directly related to the platinum backbone, as no staining and no metal shadowing was applied to the sample before observation. Thinner fibers with a width of 2 nm (Figure 2c), in close agreement with the molecular dimension determined by molecular modeling (see below), partially intertwine to form bundles of fibers with a diameter of over 4 nm, thus creating interconnected filaments (Figure 2d). At higher concentrations, no significant variation of the mean diameter is found but a higher number of interconnections are observed. The formation of these elongated fibers indicates that the self-

assembly of compound **2b** is driven by strong directional intermolecular interactions such as hydrogen bonding (observed by FTIR) and Pt···Pt interactions (observed by UV/Vis and phosphorescence spectroscopy).

Interestingly, in the solid state, complex **2c** is liquid-crystalline over a large temperature range. All the recorded X-ray diffraction (XRD) measurements (between 20 and 200 °C) are identical and show several sharp and intense small-angle reflections with reciprocal spacings in the ratios $1:\sqrt{3}:\sqrt{4}:\sqrt{7}:\sqrt{9}:\sqrt{12}:\sqrt{13}:\sqrt{16}:\sqrt{19}:\sqrt{21}$ (Figure 3). These ten

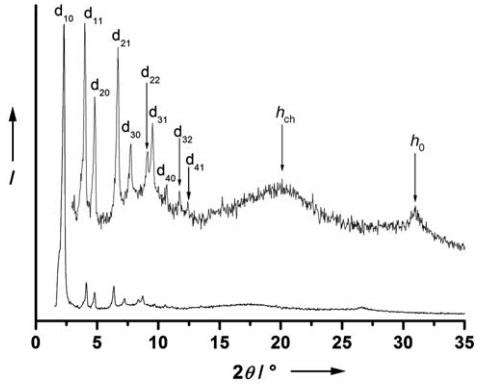

Figure 3. X-ray diffractogram of the Col_h phase of **2c** recorded at $T = 160$ °C.

small-angle peaks are most readily assigned as the (10), (11), (20), (21), (30), (22), (31), (40), (32), and (41) reflections, of a hexagonal 2D lattice with the parameter $a = 42.00$ Å (at $T =$ 160 °C; see Table S1 in the Supporting Information). The presence of these higher-order features indicates that the columnar structure is very well developed and is extended over large distances. In the wide-angle region, a broad halo, designated as h_{ch}, at 4.9–5.1 Å and another isolated sharp signal at 3.33 Å (h_0) are observed. These scattering signals can respectively be assigned to the liquid-like order of the aliphatic chains in a molten state (h_{ch}), to molecular stacking within the columns (h_0), and also to short metal–metal distances as observed in the crystalline structures of related compounds.[5,6,15]

Comparison of the stacking periodicity along the columnar axis and that along the molecular disc normal (h_0 and h, respectively) indicates that the molecules are stacked almost perpendicular to the columnar axis (see Table S1 in the Supporting Information).[16] Furthermore, the molecules likely stack in an alternated fashion in order to fill the available space between neighbors. This is also indicated by molecular dynamics (MD) simulations in which a column model was built from a periodic cylindrical cell with a 13.3-Å height (4×3.33 Å, corresponding to four stacked molecules), in keeping with the experimental X-ray data. These calculations show a good space-filling of the available volume as well as the enhancement of the microsegregation over the entire simulation experiment time, contributing to the cohesion of the columnar structure. Moreover, the model showed that the cohesion of the columns is further reinforced by Pt–Pt and Pt–alkyne interactions, as also revealed by the sharp wide-angle signal (h_0). The BF_4^- anions are located between the complexes. Snapshots of the MD experiment account for the excellent molecular packing of **2c** in the hexagonal columnar (Col_h) phase as shown in Figure 4. The size of the central rigid electron-rich core is around 2 nm, a value that is very close to the smallest width of a fiber as determined for **2b** by TEM in dilute gels.

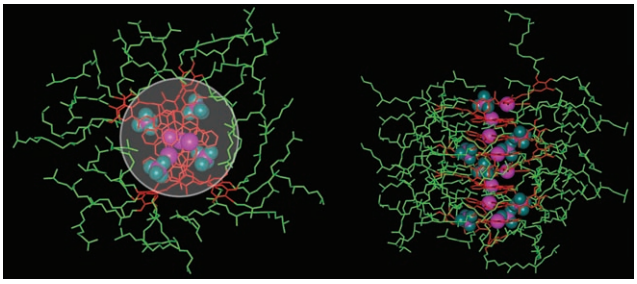

Figure 4. Snapshot showing the molecular self-assembly of **2c** into columns (polar central core shown in red, tetrafluoroborate counterion shown in blue, platinum and boron atoms shown in violet, and chains shown in green). Left: top view; right: side view (two cells). The circle has a diameter of 2 nm.

Finally, the organization of these fibrillar superstructures on well-defined crystallographic surfaces such as mica and highly ordered pyrolytic graphite (HOPG) was also investigated (note that the molecules were deposited on amorphous carbon films for the TEM investigations). A diluted gel (0.08 mmol L^{-1}) of **2b** was deposited by drop-casting on a mica substrate. As shown in Figure 5a, fibers with no apparent orientational order and an average height of 2 nm (see cross-section of Figure 5b) are clearly visible.

Interestingly, a diluted dodecane gel of compound **2b** deposited by spin-coating on freshly cleaved HOPG leads to self-assembly of molecular fibers that follow mainly the preferential crystallographic directions of the underlying HOPG substrate (Figure 5c). The threefold symmetry of the segment pattern is particularly visible at intercepts where the fibers form angles of 60° and 120° to each other. The cross-sections show the presence of two types of fibers corresponding to two different molecular heights, namely (2.0 ± 0.1) nm and (4.0 ± 0.3) nm (Figure 5d). The 2-nm high fibers can be considered to be made of single molecular layers that lie flat on the surface (Figure S1 in the Supporting Information). The 4-nm high fibers are made of two such piled up layers, with their alkyl chains still lying parallel to the surface. As can be seen from the width determined by atomic force microscopy (AFM) measurements, the fibers show a lateral extension of several tens of nanometers. As the full lateral extension of a single molecular wire is only about 3 nm, this result leads us to the conclusion that the fibers are made of monolayer and bilayer stripes that involve several molecular wires in the lateral xy direction.

The key feature of the present molecular design is the introduction of a flat Pt(terpy) luminophore to a 3,5-diacylamido framework that bears gallate-substituted derivatives. Such highly colored complexes exhibit three out-

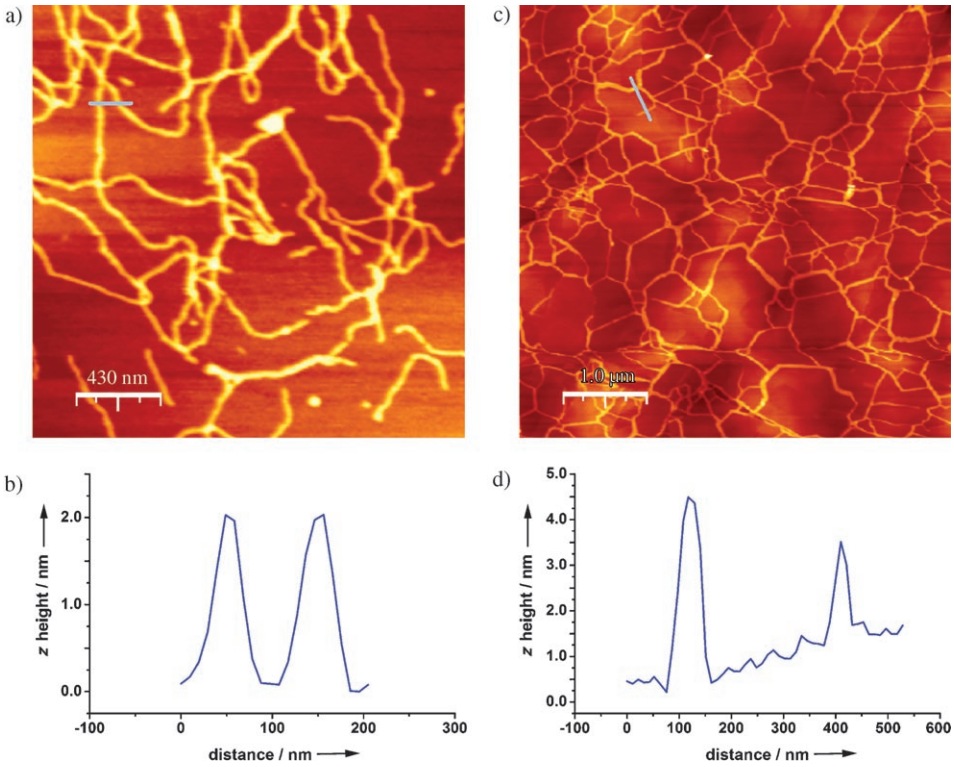

Figure 5. a) AFM tapping mode image (2.15 μm × 2.15 μm) of a dried diluted gel of **2b** in dodecane ($c = 0.08$ mmol L^{-1}) deposited on mica. b) Cross-section along the blue bar shown in part (a). c) AFM tapping mode image (5 μm × 5 μm) of a diluted gel of compound **2b** in dodecane ($c = 0.08$ mmol L^{-1}) deposited on HOPG. d) Cross-section along the blue bar shown in part (c).

standing features: 1) relative ease of synthesis and high stability; 2) strong solvatochromism and phosphorescence depending on the state of matter (solution or gel); and 3) the formation of nanofibril structures or extended columnar mesophases by switching from linear chains in **2b** to branched chains in **2c**. TEM and AFM studies confirm the presence of linear fibrils with lengths of several hundred nanometers in dodecane gels, with their 2-nm wide core consistent with complexes that strongly interacting through metal···metal (at ca. 3.6 Å) and metal···acetylide (at ca. 3.8 Å) contacts. The deep-green color and the near-infrared emission are testimony for highly aggregated complexes and effective Pt···Pt interactions. Additionally, amide functions are engaged in hydrogen bonding, which accounts for additional stabilization of the entire edifice. Fiber alignment on oriented polymer substrates would be auspicious for charge-separation devices. Studies along these lines are currently in progress.

Received: September 29, 2006
Published online: December 15, 2006

Keywords: liquid crystals · nitrogen heterocycles · organogels · platinum · self-assembly

[1] a) M. Hissler, J. E. McGarrah, W. B. Connick, D. K. Geiger, S. D. Cummings, R. Eisenberg, *Coord. Chem. Rev.* **2000**, *208*, 115–137; b) D. R. McMillin, J. J. Moore, *Coord. Chem. Rev.* **2002**, *229*, 113–121.

[2] W. Lu, B.-X. Mi, M. C. W. Chan, Z. Hui, C.-M. Che, N. Zhu, S.-T. Lee, *J. Am. Chem. Soc.* **2004**, *126*, 4958–4971.

[3] G. Arena, L. Monsu Scolaro, R. F. Pasternack, R. Romeo, *Inorg. Chem.* **1995**, *34*, 2994–3002.

[4] E. M. A. Ratilla, H. M. Brothers, N. M. Kostic, *J. Am. Chem. Soc.* **1987**, *109*, 4592–4599.

[5] W. Lu, M. C. W. Chan, N. Zhu, C.-M. Che, C. Li, Z. Hui, *J. Am. Chem. Soc.* **2004**, *126*, 7639–7651.

[6] V. W.-W. Yam, K. M.-C. Wong, N. Zhu, *J. Am. Chem. Soc.* **2002**, *124*, 6506–6507.

[7] C. Yu, K. M.-C. Wong, K. H.-Y. Chan, V. W.-W. Yam, *Angew. Chem.* **2005**, *117*, 801–804; *Angew. Chem. Int. Ed.* **2005**, *44*, 791–794.

[8] a) J. L. Sessler, W. B. Callaway, S. P. Dudek, R. W. Date, D. W. Bruce, *Inorg. Chem.* **2004**, *43*, 6650–6653; b) T. Cardinaels, J. Ramaekers, D. Guillon, B. Donnio, K. Binnemans, *J. Am. Chem. Soc.* **2005**, *127*, 17602–17603; c) S. Xiao, M. Myers, Q. Miao, S. Sanaur, K. Pang, M. L. Steigerwald, C. Nuckolls, *Angew. Chem.* **2005**, *117*, 7556–7560; *Angew. Chem. Int. Ed.* **2005**, *44*, 7390–7394; d) J. Wu, J. Li, U. Kolb, K. Müllen, *Chem. Commun.* **2006**, 48–50; e) L. A. Estroff, A. D. Hamilton, *Chem. Rev.* **2004**, *104*, 1201–1218; f) N. M. Sangeetha, U. Maitra, *Chem. Soc. Rev.* **2005**, *34*, 821–836.

[9] "Metallomesogens ": B. Donnio, D. Guillon, D. W. Bruce, R. Deschenaux in *Comprehensive Coordination Chemistry II: From Biology to Nanotechnology, Vol. 7* (Eds.: J. A. McCleverty, T. J. Meyer, M. Fujita, A. Powell), Elsevier, Oxford, **2003**, chap. 7.9, pp. 357–627.

[10] S. Takahashi, E. Murata, M. Kariya, K. Sonogashira, N. Hagihara, *Macromolecules* **1979**, *12*, 1016–1018.

[11] M. Shirakawa, N. Fujita, T. Tani, K. Kanko, S. Shinkai, *Chem. Commun.* **2005**, 4149–4151.

[12] a) F. Camerel, B. Donnio, C. Bourgogne, M. Schmutz, D. Guillon, P. Davidson, R. Ziessel, *Chem. Eur. J.* **2006**, *12*, 4261–4274; b) C.-Y. Liu, A. Fechtenkötter, M. D. Watson, K. Müllen, A. J. Bard, *Chem. Mater.* **2003**, *15*, 124–130.

[13] R. Büchner, J. S. Field, R. J. Haines, C. T. Cunningham, D. R. McMillin, *Inorg. Chem.* **1997**, *36*, 3952–3956.

[14] F. Hua, S. Kinayyigit, J. R. Cable, F. N. Castellano, *Inorg. Chem.* **2005**, *44*, 471–473, and references therein.

[15] R. Hayoun, D. K. Zhong, A. L. Rheingold, L. H. Doerrer, *Inorg. Chem.* **2006**, *45*, 6120–6122.

[16] a) D. Guillon, *Struct. Bonding (Berlin)* **1999**, *95*, 41–82; b) F. Morale, R. W. Date, D. Guillon, D. W. Bruce, R. L. Finn, C. Wilson, A. J. Blake, M. Schröder, B. Donnio, *Chem. Eur. J.* **2003**, *9*, 2484–2501.